

On the use of tuned mass dampers to suppress vortex shedding induced vibrations

Einar Strømmen[†] and Erik Hjorth-Hansen[‡]

*Department of Structural Engineering, Norwegian University of Science and Technology,
N-7491 Trondheim, Norway*

Abstract: This paper concerns computational response predictions when a tuned mass damper is intended to be used for the suppression of vortex shedding induced vibrations of e.g., a bridge deck. A general frequency domain theory is presented and its application is exemplified on a suspension bridge (where vortex shedding vibrations have been observed and where such an installation is a possible solution). Relevant load data are taken from previous wind tunnel tests. In particular, the displacement response statistics of the tuned mass damper as well as the bridge deck are obtained from time domain simulations, showing that after the installation of a TMD peak factors between three and four should be expected.

Key words: tuned mass damper; vortex shedding; dynamic response.

1. Introduction

In the design of recent Norwegian suspension bridges a wedged shaped steel box type of cross section has frequently been chosen for the bridge deck girder. With a main span between four and eight hundred meters and with only two traffic lanes plus a narrow walkway the girders on these bridges have a width to depth ratio between four and six. In spite of the wedged edges this is a fairly bluff flow obstruction rendering some of them susceptible to vortex shedding induced vibrations. Such vibrations have been observed on several of this type of suspension bridges over the last decade. Generally, the problem of vortex shedding vibrations has occurred at mean wind velocities of five to ten meters per second and usually only in fairly smooth flow. Strengthwise, the observations so far have indicated amplitudes of motion which are not likely to represent any problems regarding short term safety for any of the bridges concerned, but the long term fatigue effects are more uncertain, particularly because duration and frequency of occurrence is largely unknown. It is mainly unacceptable public confidence during such events on one bridge in particular (and ensuing alarming reports) which has demanded the owner's action into an attempt to alleviate the effects.

In connection with the planning for a 1350 m long suspension bridge across the Hardangerfjord extensive wind tunnel testing took place on a bridge girder cross section which is similar to those where vibrations have been observed today, see Hjorth-Hansen *et al.* (1993) and Strømmen & Hjorth-Hansen (1995). As presented below, section model tests took place on the problem of vortex shedding induced dynamic response and recorded at several levels of damping, allowing for the extraction of

[†] Associate Professor

[‡] Professor

valuable information regarding the fluctuating load and its motion dependency. An equally important point should be mentioned, that during this project the possibility of alleviating vortex shedding effects by use of guide vanes (around upper or lower corners) was investigated, first by CFD calculations to obtain information on favourable shape and position, and afterwards by aero-elastic section model wind tunnel tests [see Strømmen & Hjorth-Hansen (1995), where the main results are presented]. The investigations proved successful, and thus the possibility of using guide vanes to suppress vortex shedding induced bridge deck vibrations represents an attractive alternative to the use of one or several tuned mass dampers. While the use of a tuned mass damper is primarily directed at quenching the vibrations in a particular mode, the guide vanes will be effective for the reduction of excitations in any eigen-mode.

Below, the Osterøy suspension bridge has been chosen to illustrate the effectiveness of a tuned mass damper, as it is the latest case of such vibration observations. It has a main span (between towers) of 595 m. Video recordings have indicated amplitudes of motion of about 250 mm occurring at a vertical eigen-mode of four half-waves along the span between towers and with a period of about 2.5 s. This corresponds to the fourth vertical eigen-mode (second asymmetric) which according to calculations has an eigen-period of 2.55 s.

2. General theory

Several authors have presented a more or less comprehensive treatment of the effects of a tuned mass damper (below shortened TMD), of which only three have been included in the list of references below. Often, the theory has been simplified, either to a single harmonic or to a white noise type of loading. In the following, a general frequency domain treatment is presented, where the loading is described within the theory for vortex shedding induced across-wind vibrations as suggested by Vickery and Basu (1983).

Given a two-degree-of-freedom system (i.e., a minimum symbolic structural representation) with displacement components $x_1\{t\}$ and $x_2\{t\}$ and corresponding time invariant mass-, stiffness- and damping-properties M_j , K_j and C_j ($j = 1,2$), and where the element associated with $x_1\{t\}$ is subject to the load $F_1\{t\}$. The equations of motion for this system is given by :

$$\begin{bmatrix} M_1 & 0 \\ 0 & M_2 \end{bmatrix} \ddot{\mathbf{x}} + \begin{bmatrix} C_1 + C_2 & -C_2 \\ -C_2 & C_2 \end{bmatrix} \dot{\mathbf{x}} + \begin{bmatrix} K_1 + K_2 & -K_2 \\ -K_2 & K_2 \end{bmatrix} \mathbf{x} = \mathbf{F} \quad (1)$$

where $\mathbf{x} = [x_1\{t\} \ x_2\{t\}]^T$ and $\mathbf{F} = [F_1\{t\} \ 0]^T$. If the absolute degrees of freedom x_1 and x_2 are replaced by relative degrees of freedom defined as $y_1 = x_1$ and $y_2 = x_2 - x_1$, i.e.,

$$\mathbf{x} = \mathbf{T} \mathbf{y} \quad \text{where} \quad \mathbf{T} = \begin{bmatrix} 1 & 0 \\ 1 & 1 \end{bmatrix} \quad \mathbf{y} = [y_1 \ \text{and} \ y_2]^T \quad (2)$$

then, after introduction of Eq. (2) and pre-multiplication with \mathbf{T}^T , the equilibrium condition above may be written on the following form :

Table 1 Transition from two degree of freedom system to modal quantities

Two degree of freedom symbolic representation	Equivalent modal quantities	
$\begin{bmatrix} y_1 \\ y_2 \end{bmatrix}$	$\begin{bmatrix} r_z \\ r_{TMDrel} \end{bmatrix}$	where: $\begin{cases} r_z \text{ is the main system modal displ.}, \\ r_{TMDrel} \text{ is the TMD displ. relative to } r_z \end{cases}$
M_1	$M_z = m_{z0} \int_0^{L_{tot}} (\phi_z \{s\})^2 ds$	where: $\begin{cases} M_z \text{ is the modal mass,} \\ m_{z0} \text{ is evenly distributed modal mass,} \\ \phi_z \text{ is the relevant mode shape function,} \\ s \text{ is a spanwise coordinate,} \\ L_{tot} \text{ is total mode shape length} \end{cases}$
M_2	$M_{TMD} = \mu M_z$ where: μ is the mass-ratio	
C_1	$C_z = 2M_z(2\pi f_z)\zeta_z$	where: $\begin{cases} f_z \text{ is the main system eigenfrequency} \\ \text{associated with } \phi_z \text{ (with TMD absent),} \\ \zeta_z \text{ is the corresponding damping ratio} \end{cases}$
C_2	$C_{TMD} = 2M_{TMD} (2\pi f_{TMD}) \zeta_{TMD}$	where: $\begin{cases} f_{TMD} \text{ is the TMD eigen-freq.} \\ \text{(with main system fixed),} \\ \zeta_{TMD} \text{ is the TMD damping ratio} \end{cases}$
K_1 and K_2	$K_z = (2\pi f_z)^2 M_z$ and $K_{TMD} = (2\pi f_{TMD})^2 M_{TMD}$, respectively	

$$\mathbf{M} \cdot \ddot{\mathbf{y}} + \mathbf{C} \cdot \dot{\mathbf{y}} + \mathbf{K} \cdot \mathbf{y} = \mathbf{F} \quad (3)$$

$$\text{where: } \mathbf{M} = \begin{bmatrix} M_1 + M_2 & M_2 \\ M_2 & M_2 \end{bmatrix} \quad \mathbf{C} = \begin{bmatrix} C_1 & 0 \\ 0 & C_2 \end{bmatrix} \quad \text{og} \quad \mathbf{K} = \begin{bmatrix} K_1 & 0 \\ 0 & K_2 \end{bmatrix}$$

This equation is applicable to any system with a TMD attached to it where a single mode analysis is considered, if its symbolic quantities are replaced by the corresponding modal quantities. E.g., for the response calculations associated with a particular mode (whose direction of motion is indicated by a subscript co-ordinate axis z), the transition from a two degree of freedom symbolic representation to the equivalent modal quantities are given in Table 1.

The modal frequency-response-functions associated with the degrees of freedom r_z and r_{TMDrel} may then be determined from :

$$\begin{bmatrix} H_{rz}\{f\} \\ H_{TMDrel}\{f\} \end{bmatrix} = \mathbf{D}^{-1} \cdot \mathbf{d} \quad (4)$$

where : $\mathbf{D} = -(2\pi f)^2 \mathbf{M} + i(2\pi f) \mathbf{C} + \mathbf{K}$ and $\mathbf{d} = [1 \ 0]^T$, and where $i = \sqrt{-1}$. Choosing r_z to coincide with the position of the TMD along the span, i.e., at s_{TMD} , then the spectral densities $S\{f\}$ of the r_z and r_{TMDrel} displacements are given by

$$\begin{bmatrix} S_{r_z}\{f\} \\ S_{TMDrel}\{f\} \end{bmatrix} = |\phi_z\{s_{TMD}\}|^2 \cdot \begin{bmatrix} H_{r_z}^*\{f\} \cdot H_{r_z}\{f\} \\ H_{TMDrel}^*\{f\} \cdot H_{TMDrel}\{f\} \end{bmatrix} \cdot S_F\{f\} \quad (5)$$

where $\phi_z\{s_{TMD}\}$ is the mode shape value at $s = s_{TMD}$ and $S_F\{f\}$ is the spectral density of the modal load, and where $H^*\{f\}$ is the complex conjugated version of $H\{f\}$. The corresponding root mean square values (below shortened RMS) may be obtained from :

$$\begin{bmatrix} \sigma_{r_z}^2 \\ \sigma_{TMDrel}^2 \end{bmatrix} = \int_f \begin{bmatrix} S_{r_z}\{f\} \\ S_{TMDrel}\{f\} \end{bmatrix} df \quad (6)$$

The spectral density of the modal load on the primary system is given by

$$S_F\{f\} = \int_{L_{exp}} \int \phi_z\{s_a\} \cdot \phi_z\{s_b\} \cdot S_{q_z}\{f\} \cdot \sqrt{Coh_{q_z}\{\Delta s\}} \cos \Phi_{q_z} \cdot ds_a ds_b \quad (7)$$

where $S_{q_z}\{f\}$ is the spectral density of the cross-sectional loading process $q_z\{t\}$ (i.e., fluctuating load per unit length), $\sqrt{Coh_{q_z}\{\Delta s\}} \cos \Phi_{q_z}$ is the corresponding normalised co-spectrum, L_{exp} is the flow exposed length, and where s_a and s_b are symbolic representation of two arbitrary positions with separation $\Delta s = |s_a - s_b|$ along the span.

3. Dynamic load due to vortex shedding

It is in the following taken for granted that the analysis concerns across-wind vibrations due to vortex shedding of a slender (and line-like) civil engineering structure, and although the theory below is applicable to any direction of motion, it is essentially assumed that it is intended applicable for the vertical motion of a (more or less) horizontal bridge deck. It is also taken for granted that the fluctuating loading may be described within the theory developed by Vickery and Basu (1983). Then the net motion-independent cross sectional load spectrum and the corresponding co-spectrum may be expressed by

$$S_{q_z}\{f\} = \frac{(q_v D \sigma_{CL})^2}{\sqrt{\pi} f_s B} \cdot \exp\left[-\left(\frac{1-f/f_s}{B}\right)^2\right] \quad (8)$$

$$\sqrt{Coh_{q_z}\{\Delta s\}} \cos \Phi_{q_z} = \cos\left(\frac{2}{3} \frac{\Delta s}{\lambda D}\right) \cdot \exp\left[-\left(\frac{\Delta s}{3\lambda D}\right)^2\right] \quad (9)$$

where $q_v = \rho V^2 / 2$, ρ is the density of air, V is the mean wind velocity, D is the cross sectional depth (assumed constant along the span), σ_{CL} is the RMS lift coefficient, f_s is the shedding frequency ($f_s = VSt/D$, where St is the Strouhal number), B is a non-dimensional load spectrum bandwidth parameter, and λ is a non-dimensional coherence length-scale. Thus, the modal load spectrum is given by :

$$S_F\{f\} = \frac{(q_v D \sigma_{CL})^2}{\sqrt{\pi} f_s B} \exp\left[-\left(\frac{1-f/f_s}{B}\right)^2\right] \int_{L_{\text{exp}}} \int \phi_z\{s_a\} \phi_z\{s_b\} \cos\left(\frac{2\Delta s}{3\lambda D}\right) \exp\left[-\left(\frac{\Delta s}{3\lambda D}\right)^2\right] ds_a ds_b \quad (10)$$

which for most structures where the integral length scale of the vortices is small as compared to the wind exposed length L_{exp} [see Hjorth-Hansen *et al.* (1993)] may be simplified into

$$S_F\{f\} = \frac{2q_v^2 D^3 \sigma_{CL}^2 \lambda}{\sqrt{\pi} f_s B} \cdot \exp\left[-\left(\frac{1-f/f_s}{B}\right)^2\right] \cdot \int_0^{L_{\text{exp}}} (\phi\{s\})^2 ds \quad (11)$$

What then remains is to express the (negative) aerodynamic damping which is characteristic to the problem of vortex shedding induced vibrations at “lock-in”. Vickery and Basu (1983) have suggested that this effect may be described by

$$\zeta_{ae} = K_a \frac{\rho D^2}{m_{z0}} \left[1 - \left(\frac{\sigma_{rz}}{Da_L}\right)^2\right] \quad (12)$$

where K_a is an aerodynamic damping parameter (whose maximum value is $K_{a\text{max}}$), a_L is a parameter limiting “lock-in” displacements and σ_{rz} is the RMS value of structural displacement in the across-wind direction. The motion dependent total damping ratio of the main system is then given by

$$\zeta_z = \zeta_{z0} - \zeta_{ae}\{\sigma_{rz}/D\} \quad (13)$$

where ζ_{z0} is the structural eigen-damping (may also contain amplitude dependency). Thus, the calculation procedure demands iterations, because total damping is motion dependent.

Based on the theory above, a computer programme (written in Matlab) has been prepared. Because there is no automatic warning against the possibility of negative damping in the calculations of squared frequency-response-functions, the procedure of displacement iteration has been given special attention. The chosen strategy involves alternating iterations with continuously decreasing displacement steps from above (starting with Da_L) and with continuously increasing steps from below (starting with zero, or a very low value). Iterations are terminated when the difference between the two iteration branches becomes sufficiently small. An example of its application is given below.

4. Computational predictions

Computational predictions have been carried out for the possible installation of TMDs inside of the bridge deck girder hull at Osterøy suspension bridge. As shown on Fig. 1, the bridge deck has a depth of 2.5 m, limiting the available space to about 2 m.

In order to perform predictions of bridge deck girder and TMD displacements due to vortex shedding induced vibrations it is necessary to provide relevant data regarding the loading process. As mentioned above, wind tunnel tests of vortex shedding induced across-wind vibrations took place during the planning period of the Hardangerfjord bridge [Hjorth-Hansen *et al.* (1993) and Strømmen and Hjorth-Hansen (1995)], a 1325 m long suspension bridge with a bridge deck girder shapewise similar to that of the Osterøy bridge but with a width-to depth-ratio of 20/4.5., i.e., the Hardangerfjord deck girder is somewhat more bluff, and thus, its vortex shedding properties are likely to be conservative as compared to a less bluff section, but this is not considered an impediment for the application of the Hardangerfjord test data to a loading model for the case Osterøy bridge.

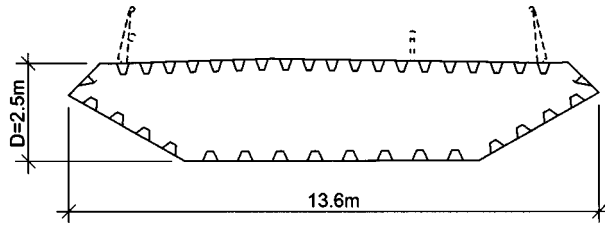


Fig. 1 Bridge deck girder on the Osterøy suspension bridge

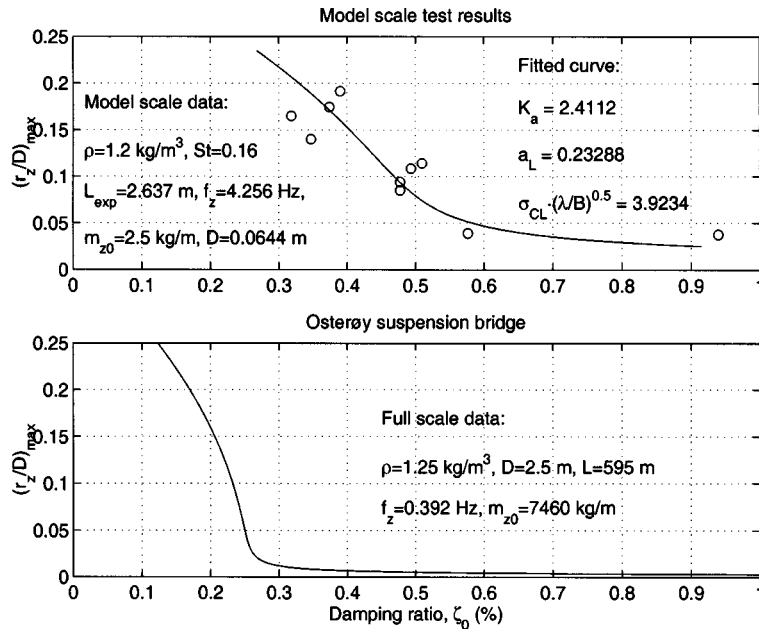


Fig. 2 Interpretation of wind tunnel test results

The interpretation and application of model scale test results is shown on Fig. 2. The open circles shown on the top graph are section model test data from the Hardangerfjord wind tunnel observations of resonant vortex shedding response at various levels of damping. (Model scale data are given on the diagram; $I_u \approx 8\%$, $I_w \approx 7.5\%$.) Least-square fitting renders: $K_a = 2.41$, $a_L = 0.233$ and $\sigma_{CL} \cdot (\lambda/B)^{0.5} = 3.92$. Applying these results to the Osterøy suspension bridge an equivalent response curve may be obtained, as shown on the lower graph of Fig. 2. Since there are full scale observations of resonant vortex shedding at $(r_z/D)_{\max} \approx 0.1$, the structural damping ratio must for these observations have been at about $\zeta_0 = 0.24\%$. This is certainly low but not unreasonable, and checking is impossible without expensive full scale tests.

What then remains is a suitable choice of the band-width parameter B and the velocity variation of K_a . The choice of these parameters will mainly affect the broad- or narrow-bandedness of the response (with respect to frequency as well as mean wind velocity), and not significantly affect the prediction of maximum RMS-values, which is of main interest in the design of a TMD (and most other cases as well). From tests the typical width of the vortex shedding response curve with respect to its variation with V is known, and based on this information B has been chosen at

a value of 0.2, and

$$K_a / K_{a \max} = [0.9 / (V/V_{cr} - 0.25)^2] \cdot \exp[-1 / (V/V_{cr} + 0.02)^{24}] - 0.18 \quad (14)$$

where $V_{cr} = Df_z / St$ (which for the relevant mode at Osterøy suspension bridge is about 6 m/s), and where the equation for the K_a -variation is limited to $0.6 \leq V / V_{cr} \leq 2.5$. Thus, a complete set of input parameters to the loading as given in Eqs. (11) and (12) has been established, as well as structural eigen-damping (inferred from observation of vortex shedding induced vibrations as described above, and assumed amplitude independent).

For the Osterøy bridge these data have been applied to investigate the effects of a tuned mass damper according to the theory presented in Chapters 2 and 3 above. Main structural parameters are given in the lower diagram of Fig. 2, apart from the mode shape that has been taken at four half-waves in accordance with observations, i.e., $\phi_z\{s\} = \sin(4\pi s / L)$. For the tuned mass damper optimal properties according to Luft (1979) have been chosen, i.e.,

$$\left. \begin{aligned} f_{TMD}/f_z &= 1 / \sqrt{1 + 1.5\mu} \\ \zeta_{TMD} &= \sqrt{0.25\mu(1 - 0.75\mu)} \end{aligned} \right\} \quad (15)$$

(These formulae have been obtained for a white-noise loading assumption, but as shown below, they are largely applicable also to the present general frequency domain solution.)

The various steps in the calculation routine is shown on Fig. 3. Top left diagram shows the modulus of the two frequency response functions, top right hand side diagram shows the load variance spectrum, lower left diagram shows the corresponding response spectra, and lower right hand side diagram shows the iteration step development of the bridge deck RMS response. The required

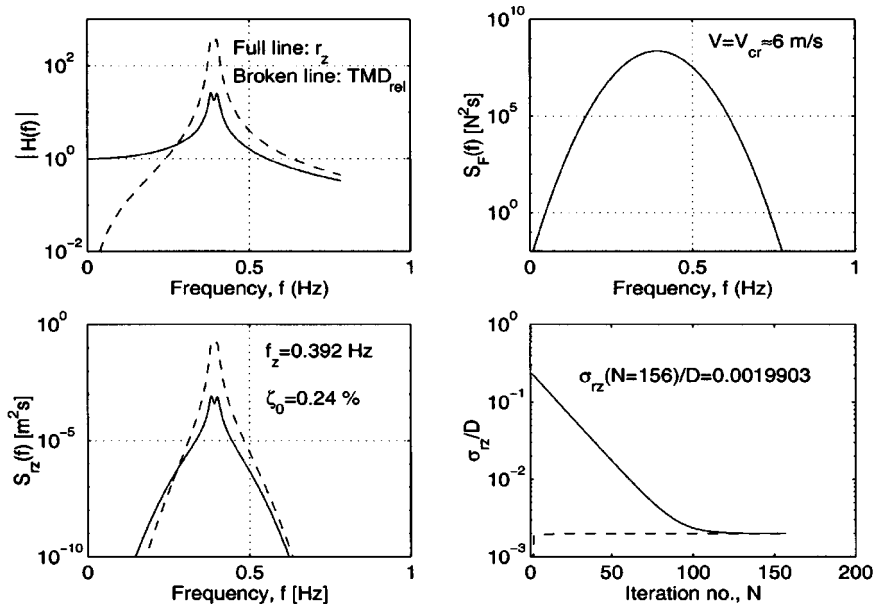


Fig. 3 The effects of a TMD (data re. Osterøy suspension bridge); $\mu = 0.3\%$, $f_{TMD} = 0.391$ Hz, $\zeta_{TMD} = 2.73\%$ and $V = V_{cr}$

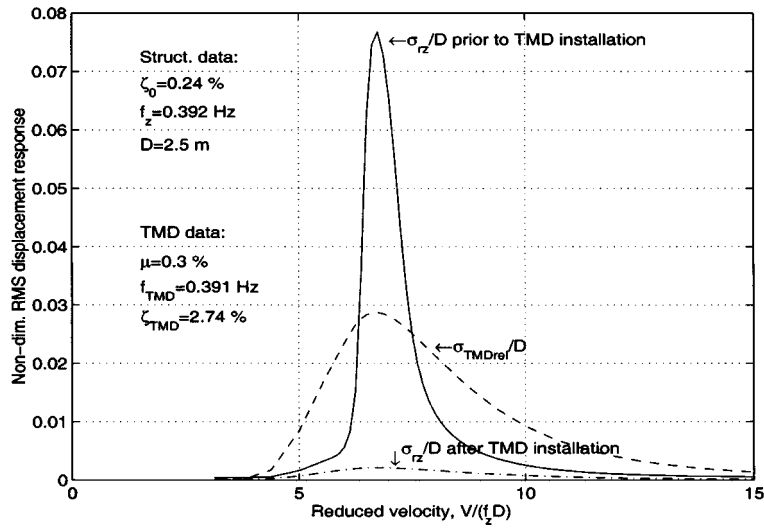


Fig. 4 Prediction of vortex shedding response before and after a TMD installation

number of iterations is in this case large (but not unduly time consuming). The reason for this is that iterations are performed on the main system modal displacement, which is very small due to the presence of the tuned mass damper.

The variation with the mean wind velocity is shown on Fig. 4 (same TMD properties as those of Fig. 3), where also the vortex shedding response prior to the TMD installation has been included. The calculations show that a TMD with a mass ratio $\mu = 0.3\%$ and optimal properties will reduce the largest RMS bridge deck displacement from about 0.2 m to 0.005 m and with a corresponding TMD displacement (relative to the bridge deck) of about 0.065 m. The results also show that the

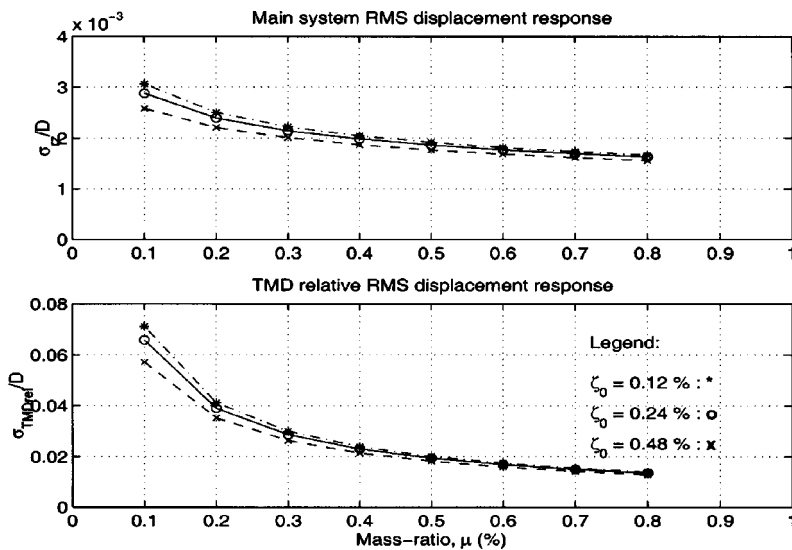


Fig. 5 Largest RMS displ. response at optimum TMD properties and various μ - settings

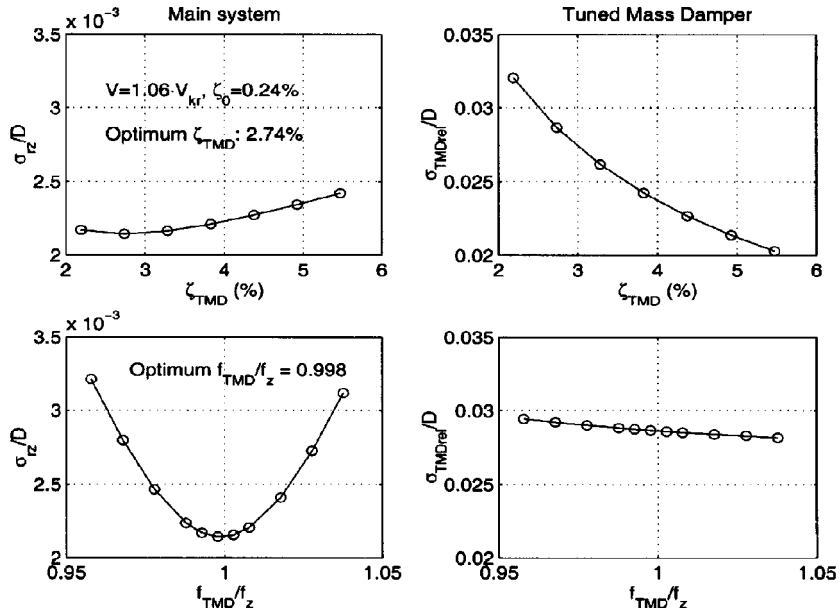


Fig. 6 Largest RMS displacement response at $\mu = 0.3\%$ and at other TMD properties different from optimum

largest dynamic response occurs at a mean wind velocity of about $1.06 \cdot V_{cr}$. The reason for this is that the Strouhal number (from model tests observed at 0.16) is here defined at onset of “lock-in”.

From a TMD design point of view the most interesting diagrams are shown on Figs. 5 and 6, where largest RMS displacements are shown for various settings of the relevant TMD properties and structural eigen-damping. As can be seen, in the presence of a mass damper tuned to properties close to optimum, the main system eigen-damping is of little importance. In the mass-ratio region between 0.3 and 0.5%, the TMD relative RMS displacement is ten to twelve times the corresponding displacements of the parent system.

It is of great interest to keep the TMD displacements within limits. At the cost of theoretical effectiveness, this can be obtained by some de-tuning of its properties. The effects of choosing TMD properties different from optimum are shown on Fig. 6, where the two upper diagrams illustrate the significance of de-tuning the damping ratio while the two lower diagrams illustrate the significance of de-tuning the frequency ratio. As can be seen, considerably lower TMD displacements can be obtained by increasing its damping, without affecting the main system displacements beyond what is acceptable.

5. Response statistics

Since the response due to vortex shedding will be more or less broad-banded after the installation of a TMD, it is of vital interest to obtain estimates of peak displacements

$$\left. \begin{aligned} r_{z, \max} &= \bar{r}_z + g_{rz} \cdot \sigma_{rz} \\ r_{TMDrel, \max} &= \bar{r}_{TMDrel} + g_{TMDrel} \cdot \sigma_{TMDrel} \end{aligned} \right\} \quad (16)$$

where \bar{r}_j are mean values (here taken at zero) and g_j are peak factors ($j = z$ or $TMDrel$), particularly

in cases where the available space for a TMD is limited. One of the main advantages with a full frequency domain solution is that it is possible to retrieve such information. Having determined the displacement response spectra $S_{r_z}\{f\}$ and $S_{TMDrel}\{f\}$ due to vortex induced vibrations, time series simulations of r_z and r_{TMDrel} may be obtained from

$$r_j\{t\} = \sum_{n=1}^N \sqrt{2S_j\{f_n\}} \Delta f_n \cos(2\pi f_n t + \theta_n + \Delta\theta_n) \quad j = r_z \text{ or } r_{TMDrel} \quad (17)$$

where N is the chosen number of frequency segments Δf_n , θ_n is a random phase angle, and $\Delta\theta_n$ is the phase lag between $r_z\{t\}$ and $r_{TMDrel}\{t\}$. Information regarding $\Delta\theta_n$ is contained in Eq. (4), and has been included in the time domain simulations. (Thus, the diagrams below show simulations of simultaneous events.)

At a mass ratio of $\mu = 0.3\%$ and a mean wind velocity of $V = 1.06 \cdot V_{cr}$ (i.e., where the largest response may be expected) such a simulation is shown on Fig. 7 (with full scale data from the Osterøy suspension bridge). As can be seen, this particular simulation rendered peak factors of about three (with $\Delta f = 0.4/200$ Hz between 0.3 and 0.5 Hz, $\Delta f = 0.4/100$ elsewhere). Other simulations may render different peak factors due to random phase. The simulation on Fig. 7 was performed at a mass-ratio of $\mu = 0.3\%$, which in this case was considered relevant for the design of a TMD. The results from simulations at mass-ratios between 0.1 and 0.8 are shown on Fig. 8. Twelve simulations have been performed at each μ -setting, from which peak factor mean values and standard deviations have been calculated. From these simulations there does not seem to be any particular trend with respect to the mass-ratio variation.

To shed more light on the peak factor statistics a total of thirty-six simulations have been performed (at $\mu = 0.3\%$). The results are presented in Fig. 9, where the data have been fitted to a Weibull distribution

$$F\{g_j\} = 1 - \exp\left[-\left(\frac{g_j - \alpha_j}{\beta_j}\right)^{\gamma_j}\right] \quad j = r_z \text{ or } r_{TMDrel} \quad (18)$$

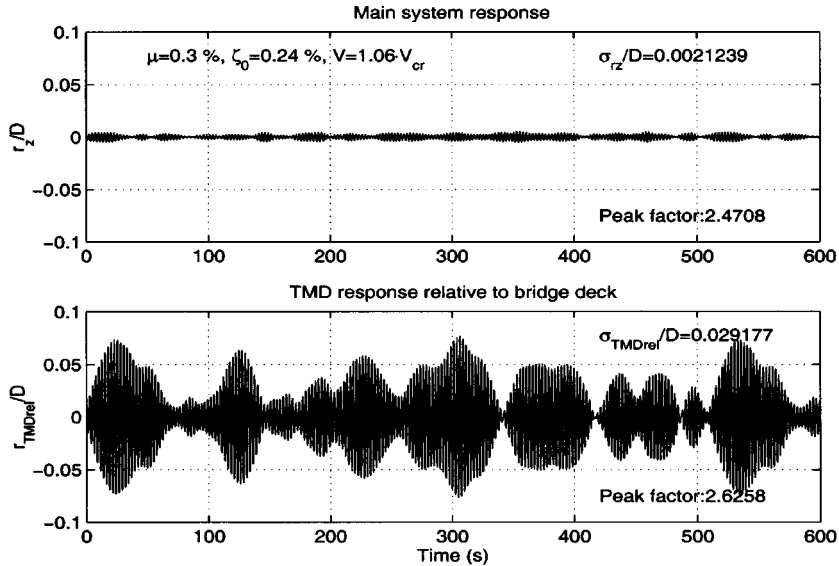


Fig. 7 Time domain response simulations, $\mu = 0.3\%$

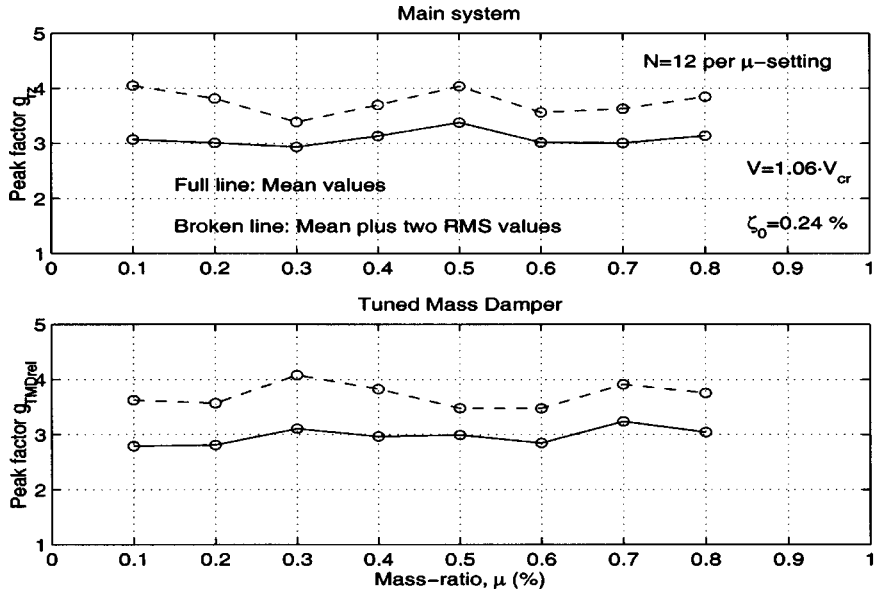


Fig. 8 Peak factors from simulations at different mass-ratios

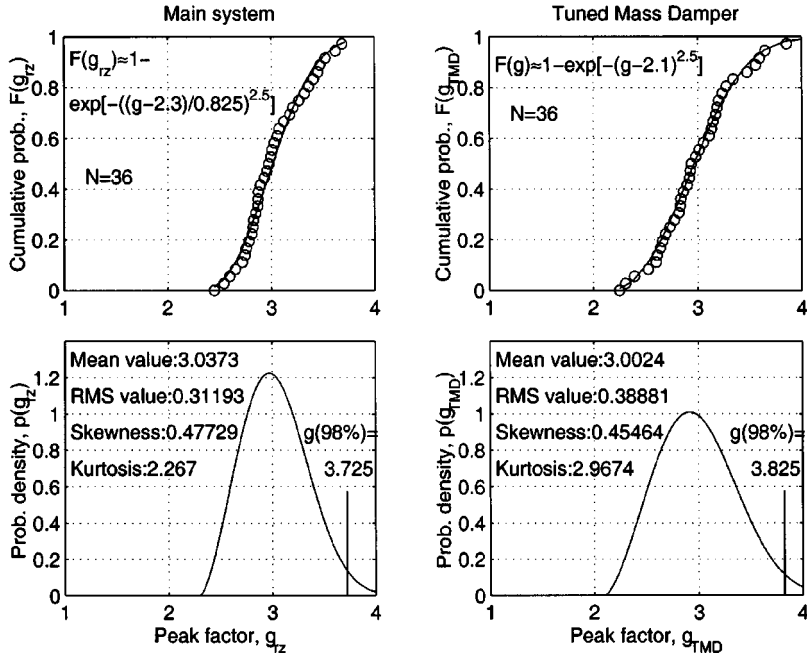


Fig. 9 Peak factor statistics ($\mu = 0.3\%$)

and where the estimated Weibull parameters α_j , β_j and γ_j are given in the upper diagrams.

The skewness and kurtosis properties of the data indicate a somewhat unsymmetrical distribution with higher probabilities on the upper tail, but with extreme value properties below what can be predicted from a Gaussian distribution. The 98% confidence intervals are given on the lower diagrams,

indicating peak factors of about 3.75 if such a criterion is chosen. However, the occurrence of events with such a peak factor are likely to be rare and of little consequence if the TMD is adequately designed to stop at a sufficiently large amplitude of motion.

6. Conclusions

In this paper a general procedure is presented for frequency domain response calculations when a tuned mass damper is intended to suppress vortex induced vibrations. The dynamic loading is described in the form of cross-spectra, and the “lock-in” effects are ascribed to a motion-dependent aerodynamic damping term. Thus, the usual simplification of a single harmonic or white noise type of loading has been avoided.

The necessary input parameters have been taken from interpretations of section model wind tunnel tests. The broad-bandedness of the motion-independent loading process was observed in wind tunnel tests on a fixed model in turbulent flow, while the motion-dependent part of the loading has been inferred from corresponding tests with an aeroelastic model.

The idea of retaining a net motion-independent loading term (see e.g., Eq. 7) seems fundamentally sound and ought to have a future in the modelling of other flow induced vibration problems where self-limiting motion-dependency is the typical behaviour (e.g., rain-wind induced cable vibrations).

Based on the interpretation of wind tunnel test results, the procedure has been applied to design predictions of a tuned mass damper for the Osterøy suspension bridge. This bridge has a main span of 595 m and an evenly distributed equivalent modal mass of about 7500 kg/m. A mass ratio of 0.3% seems a suitable choice, implying that a TMD modal mass of about 6700 kg is required. The optimum frequency ratio is close to one, and the corresponding TMD damping ratio has been calculated at 2.74%, implying a total TMD damping coefficient of about 900 Ns/m. From time domain simulations the characteristic statistics of the dynamic displacement response is presented, indicating that peak factors between three and four can be expected (with a 98% confidence interval of about 3.75). Based on a peak factor of 3.75, the maximum vortex induced modal displacements have been predicted at 0.02 m for the bridge deck and 0.37 m for the TMD.

References

- Strømmen E. and Hjorth-Hansen E. (1995), “Static and dynamic section model tests of the proposed Hardanger fjord suspension bridge”, *Proceedings of Bridges into the 21st Century*, Hong Kong, October, **1**, 251-258.
- Hjorth-Hansen E., Strømmen E., Bogunovic Jakobsen J., Brathaug H -P. and Solheim E. (1993), “Wind tunnel studies for a proposed suspension bridge across the Hardangerfjord”, *Proceedings of the 2nd European Conference on Structural Dynamics*, Trondheim, Norway, June, **2**, 1011-1018.
- Vickery, B.J. and Basu, R.I. (1983), “Across-wind vibrations of structures of circular cross-section. Part 1, Development of a mathematical model for two-dimensional conditions”, *Journal of Wind Engineering and Industrial Aerodynamics*, **12**(1), 49-73.
- Vickery, B.J. and Basu, R.I. (1983), “Across-wind vibrations of structures of circular cross-section. Part 2, Development of a mathematical model for full-scale application”, *Journal of Wind Engineering and Industrial Aerodynamics*, **12**(1), 79-97.
- Luft, R.W. (1979), “Optimal tuned mass dampers for buildings”, *Journal of the Structural Division, Proceedings of the American Society of Civil Engineers*, **105**(ST12), 2766-2772.
- McNamara, R.J. (1977), “Tuned mass dampers for buildings”, *Journal of the Structural Division, Proceedings of the American Society of Civil Engineers*, **103**(ST9), 1785-1798.
- Den Hartog, J.P. (1947). *Mechanical Vibrations*, McGraw-Hill, New York, N.Y.